

# Identification of Novel Serotonin Transporter Compounds by Virtual Screening

Mari Gabrielsen,<sup>†,○</sup> Rafał Kurczab,<sup>‡,○</sup> Agata Siwek,<sup>§</sup> Małgorzata Wolak,<sup>§</sup> Aina W. Ravna,<sup>†</sup> Kurt Kristiansen,<sup>†</sup> Irina Kufareva,<sup>∇</sup> Ruben Abagyan,<sup>∇</sup> Gabriel Nowak,<sup>§,⊥</sup> Zdzisław Chilmonczyk,<sup>||</sup> Ingebrigt Sylte,<sup>†</sup> and Andrzej J. Bojarski<sup>\*,‡</sup>

<sup>†</sup>Medical Pharmacology and Toxicology, Department of Medical Biology, Faculty of Health Sciences, UiT, The Arctic University of Norway, 9037 Tromsø, Norway

<sup>‡</sup>Department of Medicinal Chemistry, Institute of Pharmacology, Polish Academy of Sciences, 12 Smętna Street, 31-343 Kraków, Poland

<sup>§</sup>Department of Pharmacobiology, Jagiellonian University Medical College, Medyczna 9, 30-688 Kraków, Poland

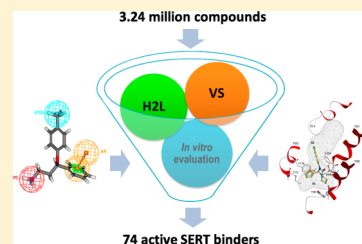
<sup>∇</sup>Skaggs School of Pharmacy and Pharmaceutical Sciences, 9500 Gilman Drive, MC 0747 La Jolla, California 92093-0747, United States

<sup>⊥</sup>Department of Neurobiology, Institute of Pharmacology, Polish Academy of Sciences, 12 Smętna Street, 31-343 Kraków, Poland

<sup>||</sup>National Medicines Institute, 30/34 Chelmska Street, 00-725 Warsaw, Poland

## Supporting Information

**ABSTRACT:** The serotonin (5-hydroxytryptamine, 5-HT) transporter (SERT) plays an essential role in the termination of serotonergic neurotransmission by removing 5-HT from the synaptic cleft into the presynaptic neuron. It is also of pharmacological importance being targeted by antidepressants and psychostimulant drugs. Here, five commercial databases containing approximately 3.24 million compounds have been screened using a combination of two-dimensional (2D) fingerprint-based and three-dimensional (3D) pharmacophore-based screening and flexible docking into multiple conformations of the binding pocket detected in an outward-open SERT homology model. Following virtual screening (VS), selected compounds were evaluated using *in vitro* screening and full binding assays and an *in silico* hit-to-lead (H2L) screening was performed to obtain analogues of the identified compounds. Using this multistep VS/H2L approach, 74 active compounds, 46 of which had  $K_i$  values of  $\leq 1000$  nM, belonging to 16 structural classes, have been identified, and multiple compounds share no structural resemblance with known SERT binders.



## INTRODUCTION

Transporters belonging to the neurotransmitter:sodium symporter (NSS) family are expressed in both eukaryotic and prokaryotic organisms.<sup>1</sup> By facilitating the translocation of a wide range of substrates across cellular membranes, the transporters play important roles in physiological processes such as maintenance of cellular osmotic pressure and neurotransmission.<sup>2,3</sup> The eukaryotic serotonin (5-hydroxytryptamine, 5-HT) transporter (SERT), together with its close relatives the noradrenaline and dopamine transporters (NET and DAT, respectively), is one of the most widely studied NSS transporters. In the central nervous system (CNS), SERT plays a pivotal role in the termination of serotonergic neurotransmission by reducing the amount of the neurotransmitter available for activation of post-synaptic 5-HT receptors.<sup>4</sup> Multiple therapeutic (e.g., antidepressants) and illicit (e.g., cocaine) drugs inhibit this reuptake, hence enhancing the serotonergic neurotransmission.<sup>4</sup>

The NSS transporters are secondary transporters that use pre-existing ion gradients as an energy source for the translocation of their substrates.<sup>3,5</sup> In the presence of sodium,

the substrate binding site (termed the S1 site), located approximately midway through the membrane, is accessible from the extracellular environment but not from the cytoplasm.<sup>6</sup> Upon substrate binding, large conformational changes occur, leading to closure of the extracellular regions and opening of the cytoplasmic parts of the transporters, resulting in the release of substrate and sodium to the cell.<sup>6</sup> However, the fine details of this alternate-access transport mechanism are not fully known. In fact, studies have suggested both 1:1 and 2:1 substrate:transporter stoichiometry.<sup>7–13</sup> In the latter scenario, it has been suggested that substrate binding to an additional site (termed S2) located in the extracellular vestibule is a prerequisite for initiation of substrate translocation from the centrally located S1 site.<sup>9,12,13</sup>

Homology modeling is an important technique in the study of NSS transporters, because, until 2013, only one member of this large family has been solved by X-ray crystallography, namely, the prokaryotic *Aquifex aeolicus* leucine transporter

**Received:** December 12, 2013

**Published:** February 12, 2014

(LeuT). In accordance with the alternate-access transport mechanism, LeuT has been crystallized in three major conformations, namely, in the outward-open (S1 site accessible from the extracellular region),<sup>7,14,15</sup> outward-occluded (S1 site inaccessible from either side of the membrane),<sup>8,10,15–21</sup> and inward-open (S1 site accessible from the cytoplasm)<sup>14</sup> conformations. Co-crystallization with substrates and non-competitive inhibitors (inhibitors occupying the S2 site)<sup>17–19</sup> stabilizes the transporter in the outward-occluded conformation.<sup>15,16</sup> In contrast, LeuT adopts an outward-open conformation when co-crystallized with the competitive inhibitor Trp.<sup>15</sup> A major breakthrough in the field of NSS transporters occurred in 2013, when a report on the first eukaryotic NSS transporter, the *Drosophila melanogaster* DAT in complex with the antidepressant nortriptyline, was published.<sup>22</sup> In addition, 12 crystal structures of LeuT with key binding pocket residues mutated to hSERT (named LeuTBAT) and co-crystallized with four classes of antidepressants were also released.<sup>23</sup> Similar to LeuT co-crystallized with Trp, the crystal structures of DAT and LeuTBAT show that the antidepressants are competitive inhibitors and stabilize the transporters in an outward-open conformation.<sup>22,23</sup>

New SERT compounds may increase our knowledge of both transport and inhibition mechanisms and could potentially lead to the development of new therapeutic drugs. One approach for identification of novel compounds is virtual screening (VS), i.e., the rapid, in silico assessment of large compound libraries, which may be performed using ligand- and/or structure-based approaches. Ligand-based VS can be employed using two-dimensional (2D) methods such as fingerprint similarity searching algorithms and three-dimensional (3D) pharmacophore models.<sup>24</sup> Ligand-based 3D pharmacophore models are generated by superimposing a set of active molecules (termed reference ligands), determining ligand conformations that can be overlaid in such a way that a maximum number of important chemical features geometrically overlap.<sup>25</sup> In comparison with ligand-based VS, which does not rely on protein 3D information, structure-based VS is performed by compound docking into either X-ray structures or homology models or by using implicit methods such as structure- or structure-docking-based pharmacophore models.<sup>24,26</sup>

Only a limited number of SERT, NET, and DAT VS studies have been published.<sup>27–38</sup> In the majority of studies, ligand-based approaches have been used, although five structure-based VS studies were recently published.<sup>30,33–35,38</sup> In these studies, docking into the central S1 site,<sup>35</sup> the S2 site,<sup>30,33,34</sup> or a putative allosteric site outside the proposed substrate translocation pathway<sup>38</sup> in outward-occluded homology models was performed. In the present study, a protocol combining ligand- and structure-based VS approaches has been used to screen five commercial databases containing ~3.24 million druglike compounds. The VS protocol comprised 2D and 3D ligand-based screening of the databases and docking of compounds into multiple conformations of the ligand binding pocket detected in an outward-open SERT homology model.<sup>39</sup> Following VS, compounds were evaluated using in vitro screening and full binding assays and the structures of active compounds were used as queries in a subsequent hit-to-lead (H2L) screening of the databases. In total, 97 compounds belonging to 22 structural classes (chemotypes) were evaluated using in vitro full binding assays. More than three of four compounds tested (74 of 97) were found to be active ( $K_i \leq 5000$  nM).

## METHODS

**Databases.** The screening and building block collections of five commercial databases were screened: Asinex,<sup>40</sup> Chem-Bridge,<sup>41</sup> ChemDiv,<sup>42</sup> Enamine,<sup>43</sup> and Life Chemicals.<sup>44</sup> Prior to screening, the databases were filtered using the Lipinski's "rule of 5" and Veber filters<sup>45,46</sup> to obtain druglike compounds.

**Reference Ligands.** The following compounds, belonging to five classes of SERT inhibitors, were used as reference ligands during the 2D and 3D ligand-based steps of the VS protocol: (S)-citalopram, desmethyl-(S)-citalopram, didesmethyl-(S)-citalopram, (S)-LU-08-052-O, (S)-LU-33-086-O, (RS)-fluoxetine, desmethyl-(RS)-fluoxetine, fluvoxamine, sertraline, desmethyl-sertraline, (RS)-venlafaxine, and O-desmethyl-(RS)-venlafaxine [SSRI/SNRI (5-HT-NE reuptake inhibitor) class], amitriptyline, clomipramine, desipramine, imipramine, protriptyline and (RS)-trimipramine [TCA class], cocaine, AB-248, AB-338,  $\beta$ -CFT, CPT-D-tartrate, RTI-31, RTI-32, RTI-55 ( $\beta$ -CIT), RTI-83, RTI-112, RTI-121, RTI-142, RTI-311 and SN-1 [3-phenyltropane class], (RS)-mazindol, (RS)-mazindane, (RS)-MAZ-10, (RS)-MAZ-85, and (RS)-MAZ-89 [mazindol class], and ADAM, 4FADAM, AFM, DAPA, DASB, IDAM, MADAM, ODAM, and 403U76 [radioligand class]. The structures and affinities of the reference ligands are shown in the Table S1 in the Supporting Information.

Individual queries were constructed for the reference ligand classes; however, because of the structural heterogeneity of the compounds in the SSRI/SNRI group, additional (S)-citalopram, sertraline, fluvoxamine, and fluoxetine/venlafaxine queries were also built. Finally, a general query was prepared from the structures of all 56 reference ligands. Hence, in the 2D and 3D steps of the VS protocol, 10 reference ligand queries were used for screening.

**VS Protocol. 2D Fingerprint-Based Screening.** To maximize the screening performance and to obtain structurally diverse compounds, 2D pharmacophore-based fingerprints and structural (hashed chemical) fingerprints were generated based on the 56 reference ligands in the 10 queries.<sup>39</sup>

Two-dimensional (2D) pharmacophore-based and structural (hashed chemical) fingerprints were generated using the GenerateMD command line tool of JChem,<sup>47</sup> using default settings. The pharmacophore-based fingerprints were constructed from the 2D molecular structures of the reference ligands by defining the collection of all-atom pharmacophore feature pairs along with their topological distances. The chemical fingerprints encoded the topological structure of the ligands into bit strings using atom type and bond type information (linear and cyclic patterns were detected).

The metrics-threshold pair was determined by three optimization iterations for each query which were performed using test sets containing compounds from a given group and randomly selected assumed inactive compounds from the ZINC database.<sup>48</sup> The optimized metrics and threshold values used during the screening can be found in Table S2 in the Supporting Information. The optimization of parametrized Tanimoto or Euclidean metrics and subsequent 2D fingerprint-based screening were performed using the Screen command line tool of JChem.<sup>47</sup>

**Basic Property and ADMET Filtering.** First, for all 56 reference ligands, the strongest basic  $pK_a$  descriptor was calculated using the Instant JChem calculator plugin.<sup>49</sup> Next, the obtained range of this parameter ( $pK_a = 3–11.5$ ) was used in the filtering of compounds that passed the 2D fingerprint-

Table 1. Novelty Analysis Results, Showing the Core Structures, SERT  $K_i$  Range (nM), and Number of Compounds in Each Chemotype (the Number of Similar Compounds, Their Potency Values (nM), and the Structure of the Most Similar Compound from the ChEMBL<sup>62</sup> or MDDR<sup>51</sup> Databases is Shown)

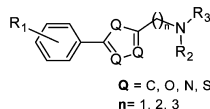
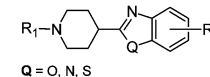
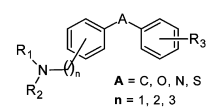
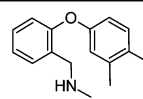
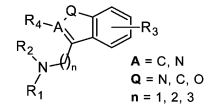
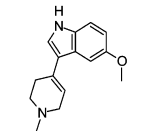
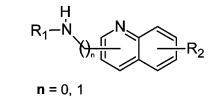
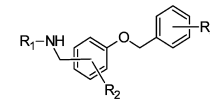
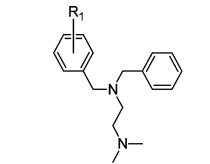
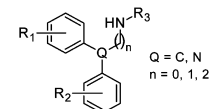
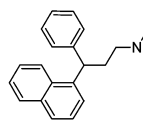
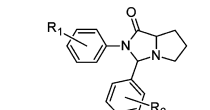
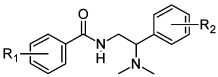
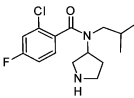
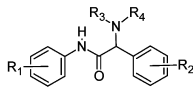
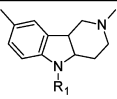
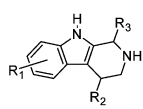
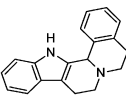
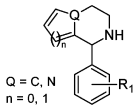
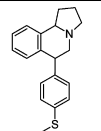
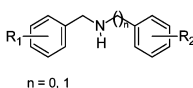
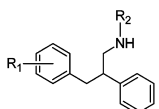
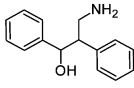
Class	Hit structure		Found in ChEMBL <sup>a</sup> or MDDR <sup>b</sup> databases	
	Core structure	$K_i$ range (nM)	Most similar structure	Similarity/Potency
C01	 <p><math>Q = C, O, N, S</math> <math>n = 1, 2, 3</math></p>	90.5 – >20 000 19 compounds	Not found	
C02	 <p><math>Q = O, N, S</math></p>	336 – >10 000 4 compounds	Not found	
C03	 <p><math>A = C, O, N, S</math> <math>n = 1, 2, 3</math></p>	926 – >20 000 – 8 compounds	 <p><math>IC_{50} = 12.8 \text{ nM}</math></p>	32 compounds with Tc: 0.50–0.68 $IC_{50}$ : 1.68–660 nM
C04	 <p><math>A = C, N</math> <math>Q = N, C, O</math> <math>n = 1, 2, 3</math></p>	1.5 – >10 000 5 compounds	 <p><math>IC_{50} = 730 \text{ nM}</math></p>	311 compounds with Tc: 0.50–0.96 $K_i$ : 0.1–10 000 nM $IC_{50}$ : 0.11–115 000 nM
C05	 <p><math>n = 0, 1</math></p>	152–1500 2 compounds	Not found	
C06		28.4–3100 10 compounds	Not found	
C07		50–1700 9 compounds	Not found	
C08	 <p><math>Q = C, N</math> <math>n = 0, 1, 2</math></p>	22.3 – >20 000 6 compounds	 <p><math>K_i = 2.4 \text{ nM}</math></p>	6 compounds with Tc: 0.51–0.76 $K_i$ : 2.4 – >10 000 nM
C09		86.1 – >20 000 5 compounds	Not found	

Table 1. continued

Class	Hit structure		Found in ChEMBL <sup>a</sup> or MDDR <sup>b</sup> databases	
	Core structure	$K_i$ range (nM)	Most similar structure	Similarity/Potency
C10		127 – >20 000 11 compounds	 $K_i = 7$ nM	81 compounds with Tc: 0.51–0.75 $K_i$ : 3 – >10 000 nM IC <sub>50</sub> : 3–400 nM
C11		56–3400 3 compounds	Not found	
C12		268–3700 3 compounds	Not found	
C13		322 – >20 000 2 compounds	 Activity = –32%	6 compounds with Tc: 0.57–0.93 Activity: –45%–(–8%)
C14	 Q = C, N n = 0, 1	2300 ± 115.5 1 compound	 $K_i = 0.01$ nM	3 compounds with Tc: 0.57–0.63 $K_i$ : 0.01–19.3 nM
C15	 n = 0, 1	2700 – >20 000 2 compounds	Not found	
C16		2300 ± 200 1 compound	 $K_i = 2730$ nM	58 compounds with Tc: 0.53–0.75 $K_i$ : 0.4–4300 nM IC <sub>50</sub> : 100–45 000 nM

<sup>a</sup>ChEMBL version 13. <sup>b</sup>MDDR version 2011.

based screening step. Compounds with unfavorable ADMET profiles were then removed from the dataset using the Schrödinger software module QikProp.<sup>50</sup> The following ADMET descriptor values were accepted: number of functional groups (rtvFG = 0–2), predicted aqueous solubility (QlogS = –6.5 to 0.5), model for gut-blood barrier (QPPCaco > 500), and predicted blood-brain coefficient (QlogBB = –3.0 to 1.2).

**3D Pharmacophore-Based Screening.** Ten ligand-based pharmacophore models were obtained using the Catalyst module of Discovery Studio (Accelrys),<sup>51</sup> employing the FAST algorithm<sup>52</sup> for generation of ligand stereoisomers and conformational sampling.

The HipHop algorithm<sup>53</sup> implemented in Catalyst<sup>51</sup> was used for pharmacophore mapping of the compounds that passed the filtering steps of the VS protocol (see above). The compounds were allowed to deviate from the pharmacophore models with maximum one feature except the positively ionizable (PI) group. Following the 3D pharmacophore-based screening, overlap analysis was performed using the Instant JChem tool from ChemAxon<sup>54</sup> in order to remove repeated structures.

**Flexible Docking.** The construction of the homology model and the 47 binding pocket conformations has been described in detail elsewhere.<sup>39</sup> The model was constructed based on the LeuT crystal structure co-crystallized with the competitive

inhibitor L-tryptophan (PDB id 3F3A)<sup>15</sup> and a comprehensive alignment of NSS transporters,<sup>1</sup> using Internal Coordinate Mechanics (ICM) software.<sup>55</sup>

The compounds were docked using a flexible docking protocol that previously has been used for reference ligands.<sup>39</sup> The protocol consisted of (1) detection of the ligand binding pocket using the ICM PocketFinder,<sup>56</sup> (2) biased-probability Monte Carlo (BPMC)<sup>57</sup> sampling and minimization of the pocket side chains in the presence of a repulsive density representing a generic ligand to prevent collapse of the binding pocket, and (3) four-dimensional (4D) docking<sup>58</sup> of fully flexible ligands into multiple pocket conformations generated during step (2). In the present study, the compounds were docked into 47 low-energy conformations of the ligand binding pocket.

The protein–ligand complexes were scored using the virtual ligand screening (VLS) scoring function of ICM.<sup>55</sup> Compounds passed the structure-based screening step when their scores were less than  $-10$  and their protonated amine moieties were located in the vicinity of D98 (TM1). The selected compounds were clustered using Molprint2D fingerprints and Tanimoto metrics using the Schrödinger software module Canvas.<sup>59</sup> In addition to the flexible docking results and the clustering of the compounds, the final selection of compounds for *in vitro* evaluation was based on financial and laboratory limitations and stock availability.

**In Vitro Evaluation of the Virtual Hits.** The assay was performed according to a previously described procedure<sup>60</sup> with slight modifications. Rat neocortical tissue was homogenized in 20 volumes of ice-cold 50 mM Tris-HCl buffer, pH 7.7 containing 150 mM NaCl and 5 mM KCl using an Ultra Turrax T25B (IKA Labortechnik, USA) homogenizer (3 pulses, each of 10 s, 19 000 rpm). The homogenate was centrifuged at 20 000 *g* for 20 min. The resulting supernatant was decanted and pellet was resuspended in the same buffer and centrifuged two more times in the same conditions. The final pellet was resuspended in an appropriate volume of buffer. [<sup>3</sup>H]-Citalopram (spec. act. 85.6 Ci/mmol, PerkinElmer) was used for 5-HT transporter labeling. Two hundred forty microliters (240  $\mu$ L) of the tissue suspension (5 mg/mL), 30  $\mu$ L of 1 nM [<sup>3</sup>H]-citalopram, and 30  $\mu$ L of the analyzed compound or 1  $\mu$ M imipramine (displacer) were incubated at 24 °C for 1 h.

During the screening experiments the compounds were analyzed at a single concentration of  $1.66 \times 10^{-6}$  M. For compounds that exhibited at least 30% [<sup>3</sup>H]-citalopram binding full competition experiments were performed in concentration range from  $10^{-9}$  to  $10^{-4}$  M. After incubation, the reaction mix was filtered immediately onto a GF/B glass fiber filter, using a 96-well FilterMate Harvester system (PerkinElmer, USA). The filter mate was dried in a microwave oven for 10 min at a power setting of 40% (700 W total power), and then it was placed in a sample bag and 10 mL of liquid scintillation cocktail was melted onto the filter. After even distribution of the scintillation cocktail, the sample bag was sealed. The radioactivity on the filter was measured using a MicroBeta TriLux 1450 scintillation counter (PerkinElmer, USA). The radioligand binding data were analyzed using iterative curve fitting routines GraphPad Prism 3.0 (GraphPad Software), which used the built-in three parameter logistic model to describe the ligand competition binding to radioligand-labeled sites. The log IC<sub>50</sub> value was estimated from the data used to obtain the  $K_i$  by applying the Cheng–Prusoff approximation.<sup>61</sup> Results are expressed as the means of at least two separate experiments.

**Hit-to-Lead (H2L) Screening.** A second *in silico* screening of the druglike subset of the five databases was performed using core structures of the compounds in chemotypes C01–C13 (see Table 1) as queries. The Instant JChem substructure searching algorithm and the symbolic query definition language module were employed.<sup>54</sup> Following the substructure screening step, the obtained compounds were screened using the basic property and ADMET filters, 3D pharmacophore models, and flexible docking procedure, as described above.

**Theoretical Novelty Analysis.** To determine the novelty of the identified compounds, the similarity between the compounds with  $K_i \leq 5000$  nM and known SERT compounds found in the MDL Drug Data Report (MDDR, version 2011)<sup>51</sup> and ChEMBL<sub>13</sub><sup>62</sup> databases was assessed using chemical hashed fingerprint and Tanimoto metric  $>0.7$  (Instant JChem).<sup>54</sup>

## RESULTS

**The VS Protocol. 2D Fingerprint-Based Screening.** In the first step of the VS protocol, screening of the druglike subsets of the Asinex,<sup>40</sup> ChemBridge,<sup>41</sup> ChemDiv,<sup>42</sup> Enamine,<sup>43</sup> and Life Chemicals<sup>44</sup> databases using 2D pharmacophore-based fingerprints and structural (hashed chemical) fingerprints and 56 reference ligands resulted in a great decrease in the number of compounds: nearly 98.5% of the druglike compounds did not pass this screening step (see Table 2).

**Table 2. Summary of the Number of Compounds That Passed Each Step of the Virtual Screening (VS) and Hit-to-Lead (H2L) Screening Protocols**

	Number of Compounds	
	VS	H2L
Lipinski's "rule of 5" and Veber filters	~ 3.24 million	
2D fingerprint-based screening	51.006	
substructure searching		8740
basic property filter	17.511	8511
ADMET filter	13.555	5030
3D pharmacophore-based screening	2293 <sup>a</sup> (5396 <sup>b</sup> )	3855 <sup>a</sup> (7791 <sup>b</sup> )
flexible docking	564 <sup>a</sup>	504 <sup>a</sup>
<i>in vitro</i> screening	202	198
<i>in vitro</i> full binding evaluation	46	51

<sup>a</sup>Unique compounds. <sup>b</sup>Stereoisomers.

**Basic Property and ADMET Filtering.** Experimental studies have suggested that D98 in transmembrane helix 1 (TM1) may anchor substrates as well as inhibitors in SERT.<sup>63–66</sup> A filter was thus employed to select compounds with basic  $pK_a$  values between 3 and 11.5, i.e., compounds containing at least one protonable nitrogen moiety. An ADMET filter was also used to remove compounds that had an unfavorable number of functional groups, and/or unfavorable aqueous solubility, blood-brain barrier, and/or gut-blood barrier coefficients.

Approximately 13 500 compounds passed the filtering steps (see Table 2).

**3D Pharmacophore-Based Screening.** The compounds were then screened using ten 3D pharmacophore models constructed based on the reference ligands. All 3D pharmacophore models contained one positively ionizable (PI) feature, one hydrophobic (HYD) feature, and one or two aromatic (AR) features (Figure 1, Figure S1 in the Supporting

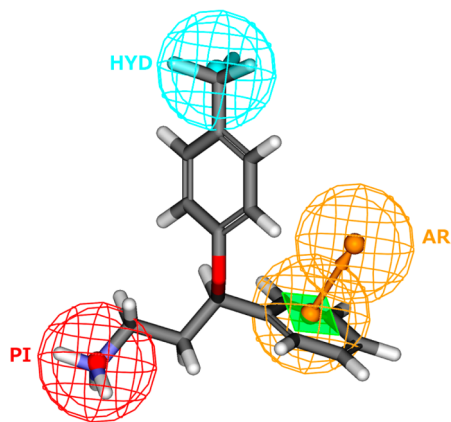


**Figure 1.** Schematic of the 3D “general hypothesis” pharmacophore model with desmethyl-(*R*)-fluoxetine mapped (PI, positive ionizable feature; AR, aromatic feature; HYD, hydrophobic feature).

Information). The simplest pharmacophore models were the general hypothesis, SSRI and TCA models, all of which contained one PI, HYD, and AR feature, and the sertraline and mazindol models, which contained one additional AR group (see Figure 1, as well as Figure S1 in the Supporting Information). The remaining pharmacophore models were more complex: the 3-phenyltropane, (*S*)-citalopram, fluoxetine/venlafaxine and fluvoxamine models possessed an additional H-bond acceptor (HBA) feature, whereas the radioligand and fluvoxamine models included an additional H-bond donor (HBD) feature and HYD region, respectively (Figure S1 in the Supporting Information). During mapping to the pharmacophore models, the compounds were allowed to deviate from the pharmacophore models with maximum one feature (except the PI feature) in order to be selected. Approximately 2300 unique compounds passed the 3D pharmacophore-based screening step of the VS protocol (see Table 2).

**Flexible Docking.** In the structure-based step of the VS protocol, a homology model generated based on an outward-open LeuT X-ray structure<sup>15</sup> was used for docking of the compounds that passed the 3D pharmacophore-based screening. In the outward-open conformation, the central S1 site of SERT was accessible from the extracellular environment and the putative inhibitor binding region constituted both the central substrate binding site (including D98 (TM1)) and extracellular vestibular regions (including the S2 site) of the transporter (Figure 2). Protein flexibility was included by docking the compounds into 47 low-energy conformations of the ligand binding pocket,<sup>39</sup> using the 4D docking approach.<sup>58</sup> A total of 564 unique compounds had scores of less than  $-10$  and a protonable nitrogen moiety in the vicinity of that of D98 (TM1) and, hence, passed the structure-based step (Table 2).

**In Vitro Radioligand Competition Binding Assays.** A total of 202 compounds from 37 chemotypes were purchased

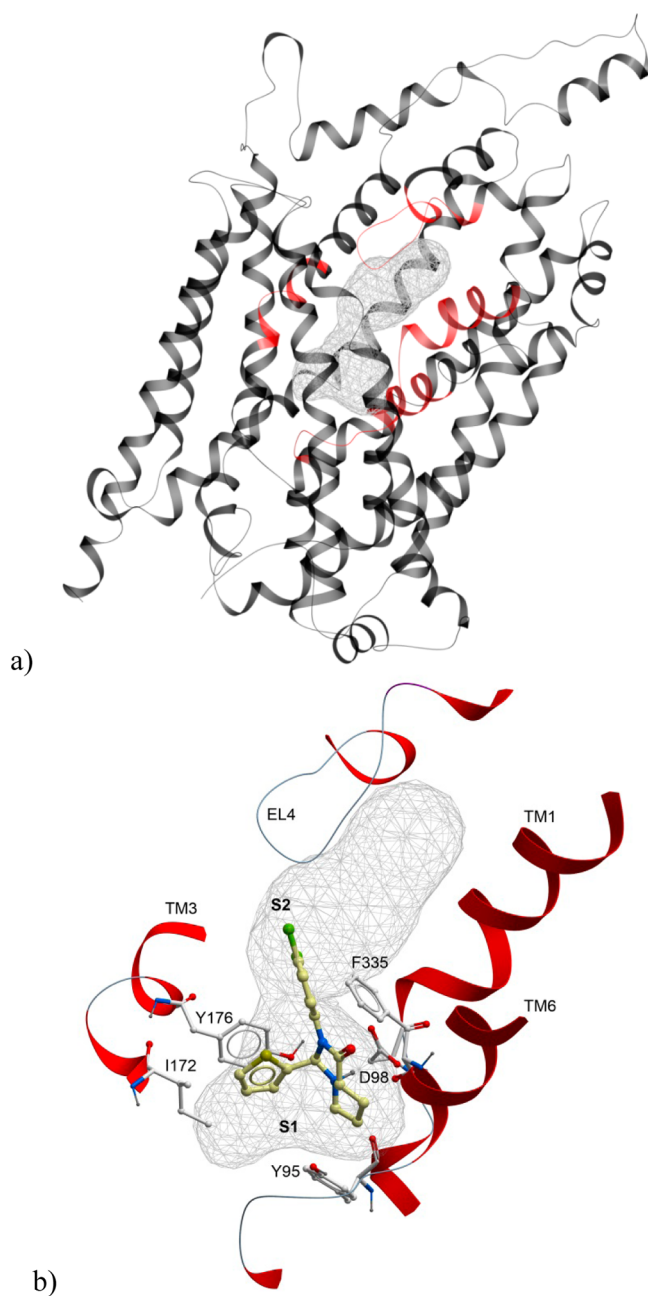


**Figure 2.** Docking results: (a) outward-open SERT homology model (gray and red ribbon representation) with ligand binding region detected by ICM PocketFinder<sup>56</sup> (gray wire mesh) and (b) docking orientation of C466-0145 (chemotype C09). Selected amino acid side chains are shown (xstick representation). For clarity, only polar hydrogen atoms are shown. The localization of the S1 and S2 binding sites are also indicated in the figure.

and screened in vitro using a [<sup>3</sup>H]-citalopram competition binding assay (see Table S3 in the Supporting Information). Twenty-three (23) of the compounds that exhibited at least 30% inhibition of [<sup>3</sup>H]-citalopram binding at a concentration of  $1.66 \times 10^{-6}$  M were further evaluated in full binding assays (see Table S4 in the Supporting Information). In addition, less-potent compounds were also selected to obtain structure–activity relationship (SAR) data and to increase the structural diversity of the evaluated compounds (Table S4 in the Supporting Information). In total, 46 compounds from 22

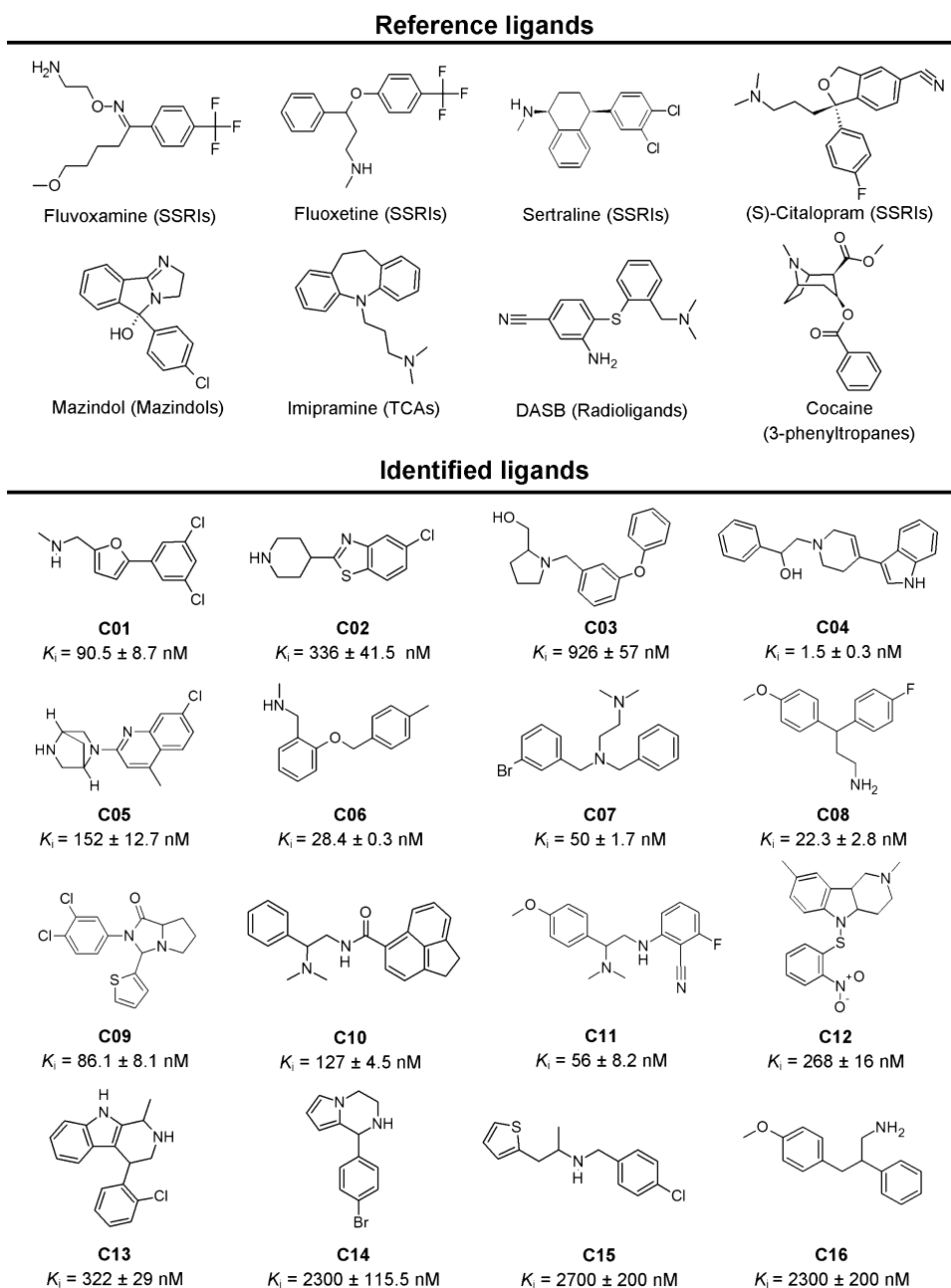


**Figure 3.** Structures of selected reference ligands and highest affinity ligand in chemotypes C01–C16, identified using the VS/H2L protocol.

chemotypes were evaluated using [<sup>3</sup>H]-citalopram competition full binding assays (see Table 2).

The results of the full binding assays revealed that 24 of the 46 compounds had  $K_i \leq 1000$  nM (see Table S4 in the Supporting Information). The affinities of 13 compounds ranged between 1000 nM and 3100 nM, whereas the remaining 9 compounds may be regarded as nonbinders ( $K_i > 10\,000$  nM) (Table S4 in the Supporting Information). Thirteen (13) chemotypes (C01–C13) contained compounds with  $K_i \leq 1000$  nM, 3 (C14–C16) had compounds with  $K_i$  between 2300 and 2700 nM, while 5 (C17–C22) only contained compounds regarded as nonbinders ( $K_i > 20\,000$  nM) (Table S4 in the Supporting Information).

**Hit-to-Lead (H2L) Screening.** To detect analogues of the compounds identified using the VS protocol, an *in silico* H2L screening of the druglike subsets of the five databases was

performed (recall Table 2). The substructure search, using the core structures of the compounds in chemotypes C01–C13 (Table 1) as queries, resulted in the detection of ~8700 analogues (see Table 2). Application of the basic property and ADMET filters reduced the number of compounds to ~5000, while 3855 unique compounds were selected during the 3D pharmacophore-based screening step and 504 unique compounds passed the flexible docking step (Table 2). In total, 198 compounds were selected for *in vitro* [<sup>3</sup>H]-citalopram screening during H2L (Table 2). Based on the results of the *in vitro* screening, 33 compounds that exhibited  $\geq 30\%$  inhibition of [<sup>3</sup>H]-citalopram binding at a concentration of  $1.66 \times 10^{-6}$  M and 18 less-potent analogues were selected for evaluation in full binding studies (see Table S4 in the Supporting Information).

Using the H2L approach, active analogues were identified in 11 of the 13 chemotypes (see Table S4 in the Supporting

Information). In total, 22 of the H2L compounds had  $K_i$  values  $\leq 1000$  nM and compounds with higher affinity than their “parent” compounds were identified in five chemotypes (chemotypes C01, C03, C04, C08 and C10; see Table S4 in the Supporting Information). The structures of the highest-affinity binder from each chemotype identified using the VS and H2L approaches are shown in Figure 3.

**Novelty Analysis.** In addition to the number and affinity of compounds identified using VS, the compound novelty is an important VS performance indicator. The structural similarity between the compounds identified in the present study and known SERT binders found in the ChEMBL<sup>62</sup> and MDDR<sup>51</sup> databases was hence determined. The results of the analysis indicated that compounds in 9 of the 16 chemotypes were structurally unrelated to known SERT ligands while the compounds in the remaining seven chemotypes showed varying degrees of similarities (Tanimoto coefficients values ranging from  $T_c = 0.50$  to  $T_c = 0.96$ ; see Table 1).

## DISCUSSION

In the present study, a multistep VS protocol (see Table 2) has been used to screen for novel, structurally diverse SERT compounds in commercially available databases. To accomplish this objective, (i) five databases containing  $\sim 3.24$  million druglike compounds were screened, (ii) multiple compounds from several structural classes of SERT inhibitors were used as reference compounds in the ligand-based steps, (iii) docking into 47 low-energy conformations of the binding pocket detected in the outward-open SERT homology model was performed in the structure-based step, and (iv) a H2L screening of the databases using the structures of the compounds identified using VS as queries was performed. In vitro evaluation of the compounds was followed by novelty analysis of the identified hits.

A combination of ligand- and structure-based VS approaches was used to screen five commercial databases, which were chosen for screening because they contain numerous, as well as a high percentage of, exclusive compounds.<sup>67</sup> The ligand-based approaches have the advantages of not heavily relying on macromolecular target information. In ligand-based VS, 3D pharmacophore models are commonly used; however, screening of large compound databases using pharmacophore models can be time-consuming.<sup>26</sup> By reducing the number of compounds in the databases prior to pharmacophore-based screening by applying a series of filters, as in the present study, the screening process can be accelerated.<sup>26</sup> Another challenge in using ligand-based pharmacophore models is that these implicit models normally only cover a limited chemical space.<sup>26</sup> In the present study, this shortcoming was addressed by constructing ten pharmacophore models based on structurally diverse groups of reference ligands and allowing partial mapping of compounds to the pharmacophore models.

By docking compounds into their 3D protein targets, steric and distance-sensitive interactions between the compounds and the protein that are not so easily explained using pharmacophore models, can be modeled.<sup>26</sup> However, experimentally determined 3D structures are not always available. Because of the lack of a SERT X-ray structure, a homology model<sup>39</sup> constructed using the prokaryotic LeuT as a template was used for docking in the present study. Despite the low overall sequence identity between LeuT and the eukaryotic NSS transporters,<sup>1</sup> LeuT is considered to be a good homology modeling template.<sup>68,69</sup> An important consideration during

homology modeling of NSS transporters, however, is which LeuT conformation to use as template, i.e., whether to use an outward-open, outward-occluded, or inward-open conformation. Because studies have indicated that most SERT ligands stabilize outward-facing conformations of the transporter,<sup>70–74</sup> the two former conformations may be good choices of templates for models used for docking. LeuT has been co-crystallized in the outward-occluded conformation with TCA and SSRI antidepressants, which, in LeuT, are noncompetitive low-affinity inhibitors.<sup>17–19</sup> In the present study, however, LeuT co-crystallized with the competitive inhibitor L-tryptophan (Trp), which stabilizes LeuT in an outward-open conformation,<sup>15</sup> was used as a template. Our previous results from docking of the reference ligands into outward-open and outward-occluded SERT models suggested that the former conformation best accommodated these compounds.<sup>39</sup> In the outward-open conformation, the central substrate binding site of SERT, containing D98 (TM1), which was indicated to be important for the binding of 5-HT and inhibitors in SERT,<sup>63–66</sup> was accessible from the extracellular environment and, hence, the putative inhibitor binding region constituted both the central substrate binding site and extracellular vestibular regions of the transporter (Figure 2). Furthermore, during preparation of the current manuscript, crystal structures of *D. melanogaster* DAT and LeuTBAT were published.<sup>22,23</sup> In support of our findings, these crystal structures show that the antidepressants indeed are competitive inhibitors of the human transporters and stabilize the transporters in outward-open conformation.<sup>22,23</sup>

In addition to the lack of protein X-ray structures, other limitations of structure-based VS may be a lack of the inclusion of protein flexibility during docking and the difficulties in scoring the protein–ligand complexes. The degrees of freedom needed to keep proteins fully flexible during docking makes such simulations computationally unfeasible and most standard docking programs use a semiflexible approach, keeping the ligands fully flexible but the proteins rigid. One method to include a degree of protein flexibility is docking into multiple receptor conformations, which is known to improve the results of VS.<sup>75,76</sup> In the present study, the compounds were docked into 47 low-energy conformations of the ligand binding pocket that had been generated prior to docking by BPMC side-chain sampling.<sup>57</sup> Docking into multiple conformations of the binding pocket was also a way of obtaining structurally diverse compounds, since studies have indicated that SERT binders most likely stabilize different outward-facing transporter conformations.<sup>70–74</sup> Furthermore, the BPMC side-chain sampling resulted in an increased distance between the aromatic amino acids of the extracellular gate (Y176 (TM3) and F335 (TM6)), hence resulting in a widening of the ligand binding pocket.<sup>39</sup> This was important for the binding of the SERT binders which are larger in size than the co-crystallized LeuT inhibitor Trp.<sup>15</sup>

In structure-based VS, scoring is used to separate potential binders from nonbinders. Empirical scoring functions such as the ICM VLS function<sup>55</sup> consist of weighted energy terms that describe known ligand binding properties (e.g., hydrogen bonding, ionic, lipophilic and aromatic interactions and the conformational entropy loss of the ligand).<sup>77</sup> However, accurate prediction of protein–ligand interactions is challenging.<sup>77</sup> The limitations of the current scoring functions may, to some degree, be addressed by evaluating the docking results using additional parameters. In the present study, the ability of the



highly scored compounds to form an ionic interaction with D98 (TM1) was used to evaluate the top-scored ligands. Analysis of the docking orientations of the compounds identified as SERT binders showed that they, when interacting with D98 (TM1), occupied the central substrate binding and lower vestibular regions (Figure 2). Halogenated moieties of the compounds were furthermore often located in the vestibular region. Interestingly, several amino acids in this region—namely, L99 (TM1), G100 (TM1), W103 (TM1), R104 (TM1), Y176 and I179 (TM3), and F335 (TM6)—have been suggested to form a halogen binding pocket (HBP) in SERT.<sup>19</sup>

The results of the *in vitro* full binding assays showed that more than 80% of the compounds evaluated were active (C01–C16;  $K_i \leq 5000$  nM) (see Table S4 in the Supporting Information). In order to find analogues of the highest-affinity binders, a H2L screening of the five databases was undertaken using the core structures of chemotypes C01–C13 as queries (recall Table 1). The H2L screening resulted in the identification of compounds that would not have been detected using the VS approach alone: comparison of the unique compounds that passed the structure-based steps of the VS and H2L protocols revealed that only 134 compounds had been selected in both approaches (results not shown).

The results of the *in vitro* full binding evaluation showed that 46 of the 97 compounds selected using the VS and H2L approaches had  $K_i$  values of  $\leq 1000$  nM (see Table S4 in the Supporting Information). The highest affinity obtained was 1.5 nM (T6125232, chemotype C04) (see Table S4 in the Supporting Information, as well as Figure 3), which is in the range of the affinities of marketed antidepressants.<sup>78,79</sup> The clustering of the identified binders furthermore showed that they were structurally diverse, belonging to 16 different structural classes (Figure 3), and the theoretical novelty analysis suggested that compounds in multiple of the chemotypes were structurally unrelated to known SERT binders in the MDDR<sup>51</sup> and ChEMBL<sup>62</sup> databases. These databases, which contain information on compounds derived primarily from the patent<sup>51</sup> and primary scientific literature,<sup>62</sup> respectively, are, however, not fully comprehensive. The novelty analysis did not reveal that T6275452 in chemotype C04 is a known SERT binder,<sup>80</sup> showing that the compound is not annotated as such in the databases. Hence, although the results indicate that multiple compounds are novel SERT binders, the results of the novelty analysis must be more rigorously evaluated.

## CONCLUSION

In the present study, virtual screening (VS) of  $\sim 3.24$  million druglike compounds has resulted in the identification of 74 active SERT binders belonging to 16 structural classes, of which 46 compounds in 13 chemotypes had  $K_i$  values of  $\leq 1000$  nM. By combining VS and hit-to-lead (H2L) approaches and selecting compounds that show varying degrees of [<sup>3</sup>H]-citalopram inhibition in the *in vitro* screening assays, compounds in multiple chemotypes can be used for SAR analysis. SAR data may be useful for elucidating the inhibition mechanism of SERT and may also be used for the development of compounds as antidepressants.

## ASSOCIATED CONTENT

### Supporting Information

Figures of the 3D ligand-based pharmacophore models and tables containing the structures of the reference ligands and

their affinities, the optimized pair metrics-thresholds used for 2D fingerprint-based screening and *in vitro* screening, and full binding assay data can be found in the Supporting Information. This material is available free of charge via the Internet at <http://pubs.acs.org>.

## AUTHOR INFORMATION

### Corresponding Author

\*Tel.: +48126623365. E-mail: [bojarski@if-pan.krakow.pl](mailto:bojarski@if-pan.krakow.pl).

### Author Contributions

○These authors contributed equally to the work.

### Author Contributions

M.G. planned the study, performed the target-based screening, analyzed the results, and wrote the paper. R.K. planned the study, performed pharmacophore modeling and ligand-based screening, analyzed the results, and reviewed the paper. A.S., M.W., and G.N. performed the *in vitro* evaluation of the compounds. A.W.R. and K.K. evaluated the 4D docking results and reviewed the paper. I.K. and R.A. contributed with 4D docking expertise and scripting, and also reviewed the paper. Z.C., I.S., and A.J.B. financed and coordinated the project, planned the studies, and reviewed the paper.

### Notes

The authors declare no competing financial interest.

## ACKNOWLEDGMENTS

The work was supported by grants from the Nevronor Program of the Research Council of Norway (Project No. 176956/V40), the Polish–Norwegian Research Fund (Grant No. PNRF-103-AI-1/07), the U.S. National Institutes of Health (Grant Nos. R01 GM071872, U01 GM094612, U54 GM094618, and RC2 LM 010994), and UiT, The Arctic University of Norway (Norway). M.G. gratefully acknowledges support and training from BioStruct, the Norwegian national graduate school in structural biology.

## ABBREVIATIONS

AR, aromatic group; DAT, dopamine transporter; HYD, hydrophobic region; H2L, hit-to-lead; ICM, Internal Coordinate Mechanics; NET, noradrenaline transporter; PI, positive ionizable group; TM, transmembrane helix; VS, virtual screening

## REFERENCES

- (1) Beuming, T.; Shi, L.; Javitch, J. A.; Weinstein, H. A comprehensive structure-based alignment of prokaryotic and eukaryotic neurotransmitter/Na<sup>+</sup> symporters (NSS) aids in the use of the LeuT structure to probe NSS structure and function. *Mol. Pharmacol.* **2006**, *70*, 1630–1642.
- (2) Saier, M. H., Jr.; Tran, C. V.; Barabote, R. D. TCDB: The Transporter Classification Database for membrane transport protein analyses and information. *Nucleic Acids Res.* **2006**, *34*, D181–186.
- (3) Krishnamurthy, H.; Piscitelli, C. L.; Gouaux, E. Unlocking the molecular secrets of sodium-coupled transporters. *Nature* **2009**, *459*, 347–355.
- (4) Iversen, L. Neurotransmitter transporters: Fruitful targets for CNS drug discovery. *Mol. Psychiatry* **2000**, *5*, 357–362.
- (5) Rudnick, G. Bioenergetics of neurotransmitter transport. *J. Bioenerg. Biomembr.* **1998**, *30*, 173–185.
- (6) Quick, M.; Yano, H.; Goldberg, N. R.; Duan, L.; Beuming, T.; Shi, L.; Weinstein, H.; Javitch, J. A. State-dependent conformations of the translocation pathway in the tyrosine transporter Tyt1, a novel neurotransmitter:sodium symporter from *Fusobacterium nucleatum*. *J. Biol. Chem.* **2006**, *281*, 26444–26454.

- (7) Piscitelli, C. L.; Gouaux, E. Insights into transport mechanism from LeuT engineered to transport tryptophan. *EMBO J.* **2012**, *31*, 228–235.
- (8) Piscitelli, C. L.; Krishnamurthy, H.; Gouaux, E. Neurotransmitter/sodium symporter orthologue LeuT has a single high-affinity substrate site. *Nature* **2010**, *468*, 1129–1132.
- (9) Shi, L.; Quick, M.; Zhao, Y.; Weinstein, H.; Javitch, J. A. The mechanism of a neurotransmitter:sodium symporter–inward release of Na<sup>+</sup> and substrate is triggered by substrate in a second binding site. *Mol. Cell* **2008**, *30*, 667–677.
- (10) Wang, H.; Elferich, J.; Gouaux, E. Structures of LeuT in bicelles define conformation and substrate binding in a membrane-like context. *Nat. Struct. Mol. Biol.* **2012**, *19*, 212–219.
- (11) Wang, H.; Gouaux, E. Substrate binds in the S1 site of the F253A mutant of LeuT, a neurotransmitter sodium symporter homologue. *EMBO Rep.* **2012**, *13*, 861–866.
- (12) Zhao, Y.; Terry, D.; Shi, L.; Weinstein, H.; Blanchard, S. C.; Javitch, J. A. Single-molecule dynamics of gating in a neurotransmitter transporter homologue. *Nature* **2010**, *465*, 188–193.
- (13) Zhao, Y.; Terry, D. S.; Shi, L.; Quick, M.; Weinstein, H.; Blanchard, S. C.; Javitch, J. A. Substrate-modulated gating dynamics in a Na<sup>+</sup>-coupled neurotransmitter transporter homologue. *Nature* **2011**, *474*, 109–113.
- (14) Krishnamurthy, H.; Gouaux, E. X-ray structures of LeuT in substrate-free outward-open and apo inward-open states. *Nature* **2012**, *481*, 469–474.
- (15) Singh, S. K.; Piscitelli, C. L.; Yamashita, A.; Gouaux, E. A competitive inhibitor traps LeuT in an open-to-out conformation. *Science* **2008**, *322*, 1655–1661.
- (16) Yamashita, A.; Singh, S. K.; Kawate, T.; Jin, Y.; Gouaux, E. Crystal structure of a bacterial homologue of Na<sup>+</sup>/Cl<sup>-</sup>-dependent neurotransmitter transporters. *Nature* **2005**, *437*, 215–223.
- (17) Singh, S. K.; Yamashita, A.; Gouaux, E. Antidepressant binding site in a bacterial homologue of neurotransmitter transporters. *Nature* **2007**, *448*, 952–956.
- (18) Zhou, Z.; Zhen, J.; Karpowich, N. K.; Goetz, R. M.; Law, C. J.; Reith, M. E.; Wang, D. N. LeuT-desipramine structure reveals how antidepressants block neurotransmitter reuptake. *Science* **2007**, *317*, 1390–1393.
- (19) Zhou, Z.; Zhen, J.; Karpowich, N. K.; Law, C. J.; Reith, M. E.; Wang, D. N. Antidepressant specificity of serotonin transporter suggested by three LeuT-SSRI structures. *Nat. Struct. Mol. Biol.* **2009**, *16*, 652–657.
- (20) Kroncke, B. M.; Horanyi, P. S.; Columbus, L. Structural origins of nitroside side chain dynamics on membrane protein alpha-helical sites. *Biochemistry* **2010**, *49*, 10045–10060.
- (21) Quick, M.; Winther, A. M.; Shi, L.; Nissen, P.; Weinstein, H.; Javitch, J. A. Binding of an octylglucoside detergent molecule in the second substrate (S2) site of LeuT establishes an inhibitor-bound conformation. *Proc. Natl. Acad. Sci. USA* **2009**, *106*, 5563–5568.
- (22) Penmatsa, A.; Wang, K. H.; Gouaux, E. X-ray structure of dopamine transporter elucidates antidepressant mechanism. *Nature* **2013**, *503*, 85–90.
- (23) Wang, H.; Goehring, A.; Wang, K. H.; Penmatsa, A.; Ressler, R.; Gouaux, E. Structural basis for action by diverse antidepressants on biogenic amine transporters. *Nature* **2013**, *503*, 141–145.
- (24) Ripphausen, P.; Nisius, B.; Peltason, L.; Bajorath, J. Quo vadis, virtual screening? A comprehensive survey of prospective applications. *J. Med. Chem.* **2010**, *53*, 8461–8467.
- (25) Wolber, G.; Seidel, T.; Bendix, F.; Langer, T. Molecule-pharmacophore superpositioning and pattern matching in computational drug design. *Drug Discovery Today* **2008**, *13*, 23–29.
- (26) Yang, S. Y. Pharmacophore modeling and applications in drug discovery: Challenges and recent advances. *Drug Discovery Today* **2010**, *15*, 444–450.
- (27) Enyedy, I. J.; Sakamuri, S.; Zaman, W. A.; Johnson, K. M.; Wang, S. Pharmacophore-based discovery of substituted pyridines as novel dopamine transporter inhibitors. *Bioorg. Med. Chem. Lett.* **2003**, *13*, 513–517.
- (28) Enyedy, I. J.; Wang, J.; Zaman, W. A.; Johnson, K. M.; Wang, S. Discovery of substituted 3,4-diphenyl-thiazoles as a novel class of monoamine transporter inhibitors through 3-D pharmacophore search using a new pharmacophore model derived from mazindol. *Bioorg. Med. Chem. Lett.* **2002**, *12*, 1775–1778.
- (29) Enyedy, I. J.; Zaman, W. A.; Sakamuri, S.; Kozikowski, A. P.; Johnson, K. M.; Wang, S. Pharmacophore-based discovery of 3,4-disubstituted pyrrolidines as a novel class of monoamine transporter inhibitors. *Bioorg. Med. Chem. Lett.* **2001**, *11*, 1113–1118.
- (30) Indarte, M.; Liu, Y.; Madura, J. D.; Surratt, C. K. Receptor-Based Discovery of a Plasmalemmal Monoamine Transporter Inhibitor via High Throughput Docking and Pharmacophore Modeling. *ACS Chem. Neurosci.* **2010**, *1*, 223–233.
- (31) Kim, C. Y.; Mahaney, P. E.; McConnell, O.; Zhang, Y.; Manas, E.; Ho, D. M.; Deecher, D. C.; Trybulski, E. J. Discovery of a new series of monoamine reuptake inhibitors, the 1-amino-3-(1H-indol-1-yl)-3-phenylpropan-2-ols. *Bioorg. Med. Chem. Lett.* **2009**, *19*, 5029–5032.
- (32) Kiss, R.; Sandor, M.; Gere, A.; Schmidt, E.; Balogh, G. T.; Kiss, B.; Molnar, L.; Lemmen, C.; Keseru, G. M. Discovery of novel histamine H4 and serotonin transporter ligands using the topological feature tree descriptor. *J. Chem. Inf. Model.* **2012**, *52*, 233–242.
- (33) Manepalli, S.; Geffert, L. M.; Surratt, C. K.; Madura, J. D. Discovery of novel selective serotonin reuptake inhibitors through development of a protein-based pharmacophore. *J. Chem. Inf. Model.* **2011**, *51*, 2417–2426.
- (34) Nolan, T. L.; Lapinsky, D. J.; Talbot, J. N.; Indarte, M.; Liu, Y.; Manepalli, S.; Geffert, L. M.; Amos, M. E.; Taylor, P. N.; Madura, J. D.; Surratt, C. K. Identification of a novel selective serotonin reuptake inhibitor by coupling monoamine transporter-based virtual screening and rational molecular hybridization. *ACS Chem. Neurosci.* **2011**, *2*, 544–552.
- (35) Schlessinger, A.; Geier, E.; Fan, H.; Irwin, J. J.; Shoichet, B. K.; Giacomini, K. M.; Sali, A. Structure-based discovery of prescription drugs that interact with the norepinephrine transporter, NET. *Proc. Natl. Acad. Sci. USA* **2011**, *108*, 15810–15815.
- (36) Wang, S.; Sakamuri, S.; Enyedy, I. J.; Kozikowski, A. P.; Deschoux, O.; Bandyopadhyay, B. C.; Tella, S. R.; Zaman, W. A.; Johnson, K. M. Discovery of a novel dopamine transporter inhibitor, 4-hydroxy-1-methyl-4-(4-methylphenyl)-3-piperidyl 4-methylphenyl ketone, as a potential cocaine antagonist through 3D-database pharmacophore searching. Molecular modeling, structure-activity relationships, and behavioral pharmacological studies. *J. Med. Chem.* **2000**, *43*, 351–360.
- (37) MacDougall, I. J.; Griffith, R. Pharmacophore design and database searching for selective monoamine neurotransmitter transporter ligands. *J. Mol. Graph. Model.* **2008**, *26*, 1113–1124.
- (38) Kortagere, S.; Fontana, A. C.; Rose, D. R.; Mortensen, O. V. Identification of an allosteric modulator of the serotonin transporter with novel mechanism of action. *Neuropharmacology* **2013**, *72*, 282–290.
- (39) Gabrielsen, M.; Kurczab, R.; Ravna, A. W.; Kufareva, I.; Abagyan, R.; Chiltonczyk, Z.; Bojarski, A. J.; Sylte, I. Molecular mechanism of serotonin transporter inhibition elucidated by a new flexible docking protocol. *Eur. J. Med. Chem.* **2012**, *47*, 24–37.
- (40) Asinex Home Page, [www.asinex.com](http://www.asinex.com) (accessed 2010).
- (41) ChemBridge Home Page, [www.chembridge.com](http://www.chembridge.com) (accessed 2010).
- (42) ChemDiv Home Page, [www.chemdiv.com](http://www.chemdiv.com) (accessed 2010).
- (43) Enamine Home Page, [www.enamine.net](http://www.enamine.net) (accessed 2010).
- (44) Life Chemicals Home Page, [www.lifechemicals.com](http://www.lifechemicals.com) (accessed 2010).
- (45) Lipinski, C. A.; Lombardo, F.; Dominy, B. W.; Feeney, P. J. Experimental and computational approaches to estimate solubility and permeability in drug discovery and development settings. *Adv. Drug Delivery Rev.* **2001**, *46*, 3–26.
- (46) Veber, D. F.; Johnson, S. R.; Cheng, H. Y.; Smith, B. R.; Ward, K. W.; Kopple, K. D. Molecular properties that influence the oral bioavailability of drug candidates. *J. Med. Chem.* **2002**, *45*, 2615–2623.

- (47) JChem version 5.3.1, ChemAxon (<http://www.chemaxon.com>).
- (48) Irwin, J. J.; Shoichet, B. K. ZINC—A free database of commercially available compounds for virtual screening. *J. Chem. Inf. Model.* **2005**, *45*, 177–182.
- (49) Marvin, version 5.3.1, ChemAxon (<http://www.chemaxon.com>).
- (50) QikProp, version 3.2; Schrödinger LLC: New York, 2010.
- (51) D.S.M.E., Release 2.5; Accelrys Software, Inc.: San Diego, CA, 2010.
- (52) Beutler, T. C.; Dill, K. A. A fast conformational search strategy for finding low energy structures of model proteins. *Protein Sci.* **1996**, *5*, 2037–2043.
- (53) Barnum, D.; Greene, J.; Smellie, A.; Sprague, P. Identification of common functional configurations among molecules. *J. Chem. Inf. Comput. Sci.* **1996**, *36*, 563–571.
- (54) Instant JChem, version 5.3.1; ChemAxon (<http://www.chemaxon.com>).
- (55) Abagyan, R.; Totrov, M.; Kuznetsov, D. ICM—A new method for protein modeling and design: Applications to docking and structure prediction from the distorted native conformation. *J. Comput. Chem.* **1994**, *15*, 488–506.
- (56) An, J.; Totrov, M.; Abagyan, R. Pocketome via comprehensive identification and classification of ligand binding envelopes. *Mol. Cell Proteomics* **2005**, *4*, 752–761.
- (57) Abagyan, R.; Totrov, M. Biased probability Monte Carlo conformational searches and electrostatic calculations for peptides and proteins. *J. Mol. Biol.* **1994**, *235*, 983–1002.
- (58) Bottegioni, G.; Kufareva, I.; Totrov, M.; Abagyan, R. Four-dimensional docking: A fast and accurate account of discrete receptor flexibility in ligand docking. *J. Med. Chem.* **2009**, *52*, 397–406.
- (59) Canvas software; Schrödinger LLC: New York, 2010.
- (60) Wrobel, M. Z.; Chodkowski, A.; Herold, F.; Gomolka, A.; Kleps, J.; Mazurek, A. P.; Plucinski, F.; Mazurek, A.; Nowak, G.; Siwek, A.; Stachowicz, K.; Slawinska, A.; Wolak, M.; Szewczyk, B.; Satala, G.; Bojarski, A. J.; Turlo, J. Synthesis and biological evaluation of novel pyrrolidine-2,5-dione derivatives as potential antidepressant agents. Part 1. *Eur. J. Med. Chem.* **2013**, *63*, 484–500.
- (61) Cheng, Y.; Prusoff, W. H. Relationship between the inhibition constant ( $K_1$ ) and the concentration of inhibitor which causes 50% inhibition ( $I_{50}$ ) of an enzymatic reaction. *Biochem. Pharmacol.* **1973**, *22*, 3099–3108.
- (62) Gaulton, A.; Bellis, L. J.; Bento, A. P.; Chambers, J.; Davies, M.; Hersey, A.; Light, Y.; McGlinchey, S.; Michalovich, D.; Al-Lazikani, B.; Overington, J. P. ChEMBL: A large-scale bioactivity database for drug discovery. *Nucleic Acids Res.* **2012**, *40*, D1100–D1107.
- (63) Andersen, J.; Olsen, L.; Hansen, K. B.; Taboureau, O.; Jorgensen, F. S.; Jorgensen, A. M.; Bang-Andersen, B.; Egebjerg, J.; Stromgaard, K.; Kristensen, A. S. Mutational mapping and modeling of the binding site for (S)-citalopram in the human serotonin transporter. *J. Biol. Chem.* **2010**, *285*, 2051–2063.
- (64) Barker, E. L.; Moore, K. R.; Rakhshan, F.; Blakely, R. D. Transmembrane domain I contributes to the permeation pathway for serotonin and ions in the serotonin transporter. *J. Neurosci.* **1999**, *19*, 4705–4717.
- (65) Celik, L.; Sinning, S.; Severinsen, K.; Hansen, C. G.; Moller, M. S.; Bols, M.; Wiborg, O.; Schiott, B. Binding of serotonin to the human serotonin transporter. Molecular modeling and experimental validation. *J. Am. Chem. Soc.* **2008**, *130*, 3853–3865.
- (66) Sinning, S.; Musgaard, M.; Jensen, M.; Severinsen, K.; Celik, L.; Koldso, H.; Meyer, T.; Bols, M.; Jensen, H. H.; Schiott, B.; Wiborg, O. Binding and orientation of tricyclic antidepressants within the central substrate site of the human serotonin transporter. *J. Biol. Chem.* **2010**, *285*, 8363–8374.
- (67) Chuprina, A.; Lukin, O.; Demoiseaux, R.; Buzko, A.; Shivanyuk, A. Drug- and lead-likeness, target class, and molecular diversity analysis of 7.9 million commercially available organic compounds provided by 29 suppliers. *J. Chem. Inf. Model.* **2010**, *50*, 470–479.
- (68) Dodd, J. R.; Christie, D. L. Selective amino acid substitutions convert the creatine transporter to a gamma-aminobutyric acid transporter. *J. Biol. Chem.* **2007**, *282*, 15528–15533.
- (69) Stockner, T.; Montgomery, T. R.; Kudlacek, O.; Weissensteiner, R.; Ecker, G. F.; Freissmuth, M.; Sitte, H. H. Mutational analysis of the high-affinity zinc binding site validates a refined human dopamine transporter homology model. *PLoS Comput. Biol.* **2013**, *9*, e1002909.
- (70) Forrest, L. R.; Zhang, Y. W.; Jacobs, M. T.; Gesmonde, J.; Xie, L.; Honig, B. H.; Rudnick, G. Mechanism for alternating access in neurotransmitter transporters. *Proc. Natl. Acad. Sci. U.S.A.* **2008**, *105*, 10338–10343.
- (71) Tavoulari, S.; Forrest, L. R.; Rudnick, G. Fluoxetine (Prozac) binding to serotonin transporter is modulated by chloride and conformational changes. *J. Neurosci.* **2009**, *29*, 9635–9643.
- (72) Torres-Altora, M. I.; Kuntz, C. P.; Nichols, D. E.; Barker, E. L. Structural analysis of the extracellular entrance to the serotonin transporter permeation pathway. *J. Biol. Chem.* **2010**, *285*, 15369–15379.
- (73) Zhang, Y. W.; Rudnick, G. The cytoplasmic substrate permeation pathway of serotonin transporter. *J. Biol. Chem.* **2006**, *281*, 36213–36220.
- (74) Rothman, R. B.; Baumann, M. H.; Blough, B. E.; Jacobson, A. E.; Rice, K. C.; Partilla, J. S. Evidence for noncompetitive modulation of substrate-induced serotonin release. *Synapse* **2010**, *64*, 862–869.
- (75) Rueda, M.; Totrov, M.; Abagyan, R. ALiBERO: Evolving a team of complementary pocket conformations rather than a single leader. *J. Chem. Inf. Model.* **2012**, *52*, 2705–2714.
- (76) Totrov, M.; Abagyan, R. Flexible ligand docking to multiple receptor conformations: A practical alternative. *Curr. Opin. Struct. Biol.* **2008**, *18*, 178–184.
- (77) Huang, S. Y.; Grinter, S. Z.; Zou, X. Scoring functions and their evaluation methods for protein–ligand docking: Recent advances and future directions. *Phys. Chem. Chem. Phys.* **2010**, *12*, 12899–12908.
- (78) Owens, M. J.; Knight, D. L.; Nemeroff, C. B. Second-generation SSRIs: Human monoamine transporter binding profile of escitalopram and R-fluoxetine. *Biol. Psychiatry* **2001**, *50*, 345–350.
- (79) Owens, M. J.; Morgan, W. N.; Plott, S. J.; Nemeroff, C. B. Neurotransmitter receptor and transporter binding profile of antidepressants and their metabolites. *J. Pharmacol. Exp. Ther.* **1997**, *283*, 1305–1322.
- (80) Adkins, E. M.; Barker, E. L.; Blakely, R. D. Interactions of tryptamine derivatives with serotonin transporter species variants implicate transmembrane domain I in substrate recognition. *Mol. Pharmacol.* **2001**, *59*, 514–523.